RSC Advances

ROYAL SOCIETY OF CHEMISTRY

www.rsc.org/advances

Enhancing photoluminescence (PL) of single layer (1L) MoS_2 is critical to its application as thinnest light-emission material. In this report, we show that the PL intensity of 1L MoS_2 can be greatly enhanced by physorbtion of H_2O_2 molecules that act as *p*-type dopants. By using toluene to form the sandwiched structure of H_2O_2/1L-MoS_2/toluene, the PL intensity of 1L MoS_2 can be enhanced up to 27.4 times. Our research proposes a simple but effective method to enhance the light emitting properties of 1L MoS_2.

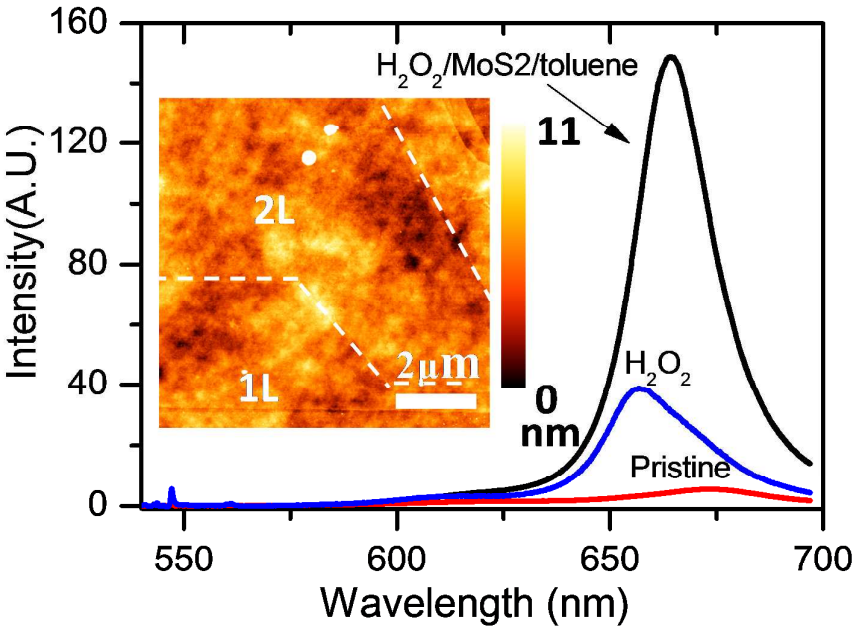

Tuning Photoluminescence of single-layer MoS_2 using H_2O_2

Weitao Su[1, 2*], Honglei Dou[1], Jinwei Li[1], Dexuan Huo[1,*], Ning Dai[2], Li Yang[3]

[1]Institute of Materials Physics, Hangzhou Dianzi University, 310018, Hangzhou, China

[2]Ningbo Institute of Materials Technology & Engineering, Chinese Academy of Sciences, 315201, Ningbo, China

[3] Department of Chemistry, Xi'an Jiaotong-Liverpool University, 215123, Suzhou, China

Corresponding author: Weitao Su, suweitao@hdu.edu.cn;
Dexuan Huo, dxhuo@hdu.edu.cn
Telephone & Fax: +86-571-86878539

Abstract Enhancing photoluminescence (PL) of single-layer (1L) MoS_2 is critical to its application as thinnest light-emission material. In this report, we show that the PL intensity of 1L-MoS_2 can be enhanced by 8 times using physisorption of H_2O_2 molecules as *p*-type dopants. By using toluene to form the sandwiched structure of H_2O_2/1L-MoS_2/toluene, the PL intensity of 1L-MoS_2 can be enhanced up to 27.4 times. Our research proposes a simple but effective method to enhance the light emitting properties of 1L-MoS_2.

1. Introduction

In recent years, as the thinnest optoelectronic material, single-layer MoS_2 has drew much attention in various potential applications, such as light emitting[1, 2], photon-detection[3-5], energy harvesting[2] ,etc. Bulk MoS_2 crystal is composed by periodic layers bonded together by Van der Waals force. Within each period a layer of molybdenum atoms are sandwiched between two layers of sulphur atoms[6]. When the layer number is reduced from multilayer to 1L, the band structure of MoS_2 transits from indirect (band gap~1.1eV)[7] to direct band (band gap~2.0eV). Large band gap and high exciton binding energy (~600meV)[8] of 1L-MoS_2 result into strong light emission in red light (620-680nm) even at room temperature[9]. However, in contrast

to other widely used rare earth compounds [10, 11], the PL quantum efficiency of pristine 1L-MoS_2 is too low (0.4%)[6] to meet the requirements of light emitting devices[10, 11]. Hence various methods such as localized surface plasmon(LSP)[12] resonance and molecule doping[13-15] etc., had been proposed to enhance the PL intensity and tune the band position. Doping using *p*-type molecules, such as H_2O[15], oxygen[14, 15], adzobenzene[16], etc., allows to enhance the PL intensity of 1L-MoS_2 by up to tens of times. Theoretically, the PL enhancement using these p-type molecule is attributed to the weakened the Auger-related non-radiative recombination, which is induced by the reduced electron concentration of 1L-MoS_2 with the presence of p-type dopants[15]. However, although H_2O and oxygen molecules are p-type molecules[14, 15], adsorbtion of such molecules from ambient condition is unable to enhance the PL intensity of 1L-MoS_2[14]. Therefore activation process like vacuum annealing is critical to enhance PL of 1L-MoS_2 with such molecules [14, 15]. Using a *p*-type molecule with strong oxidability or good contact with MoS_2 , such as astetracyanoquino- dimethane TCNQ[13], such activation process may be unnecessary and the preparation process of 1L-MoS_2 with high PL yield can be greatly simplified. With strong oxidability than H_2O and oxygen, H_2O_2 can be a useful p-type dopant that may effectively enhances the light emission of 1L-MoS_2 without activation process. However, to our best knowledge, few reports concerned on this topic had been published yet.

In order to obtain effective PL enhancement, the dose of H_2O_2 molecules needs to be carefully controlled due to high reactivity of H_2O_2 molecules. If the

concentration of H_2O_2 is high enough to react with MoS_2 following the equation $MoS_2+7H_2O_2=MoO_3+7H_2O+2SO_2$, the lattice of 1L-$MoS_2$ may partially or totally react into MoO_3 and consequently the PL of 1L-MoS_2 is quenched. Therefore, low concentration of H_2O_2 molecules is desirable to maintain intact lattice of 1L-MoS_2 so that PL enhancement can be obtained. In this study, we employed two different methods, i.e. physisorption of H_2O_2 molecules on SiO_2 substrates (method Ⅰ of Figure. 1) and spin-coating of H_2O_2 molecules with low concentration (method Ⅱ of Figure.1). It's expected that with same concentration of H_2O_2 solutions, the dose of H_2O_2 molecules prepared by physisorption (method Ⅰ) is much lower than that of spin-coating (method Ⅱ). It's shown for the first time that the PL intensity of 1L-MoS_2 can be greatly enhanced by using H_2O_2 with optimized dose. Much stronger enhancement than that of H_2O_2/1L-MoS_2 is observed on a new sandwiched structure of H_2O_2/1L-MoS_2/toluene. Our research is expected to benefit 1L-MoS_2 in the application of light-emission devices with high performance.

2. Details of experiment and calculation

Two different methods, i.e. absorbtion method(method Ⅰ, top panel of Figure 1) and spin-coating method (method Ⅱ, bottom panel of Figure 1), were used to prepare H_2O_2 treated samples. In method Ⅰ, SiO_2(300nm)/silicon substrates firstly were ultrasonically rinsed in H_2O_2 solution with different concentrations (0.3%, 3%,30%) for 10mins. Then the substrates were drained and rapidly dried at room temperature, which left a thin layer of H_2O_2 molecules adsorbed on SiO_2 surface. After mechanical exfoliation, the H_2O_2 molecules physisorbed on SiO_2 surface were

sandwiched between SiO_2 and 1L-MoS_2. In method Ⅱ, MoS_2 flakes were firstly exfoliated on clean SiO_2(300nm)/Si substrates, then 10ul of H_2O_2 solutions with different concentrations of (0.3%, 3%,30%) were spin coated with spin speed of 6000-8000 rpm. Then the samples were flushed with deionized water immediately after spin-coating. In the preparation of H_2O_2/1L-MoS_2/toluene samples, H_2O_2/1L-MoS_2 samples were firstly prepared using method Ⅰ, and immediately spin coated with different concentration(10^{-6}, 10^{-9}mol/l) of toluene/ethanol solution.

The modified 1L-MoS_2 flakes were identified using optical microscope. PL and Raman spectra were measured on a Raman spectroscopy (Senterra, Bruker) in back scattering mode. A Nd:YAG double frequency laser (532nm) was used as excitation source. An 100x objective lens with N.A.=0.9 was used for excitation and collection of PL and Raman signals. A low laser power as 0.2mW at the sample was used to avoid overheating. Gratings with 400 grooves/mm and 1200 grooves/mm were used to obtain PL and Raman spectra, respectively. Exposure time of 10s and 120s were used for PL and Raman measurements, respectively. An atomic force microscope (AFM, Agilent 5500) operated at tapping mode was used to measure topographic images of 1L-MoS_2.

The geometry optimization and electronic structure calculations of 1L-MoS_2 before and after adsorbtion of H_2O_2 molecules were performed using the self-consistent full potential linear augmented plane wave method implemented in WIEN2k code[17] within the density functional theory(DFT) with a conventional exchange- correlation Perdew, Burke, and Ernzerhof (PBE) potential. In the

calculation of electronic properties, a 5×5×1 super cell was used. The effect of spin-orbit coupling was considered in our calculations. The value of $K_{max}\times R_{MT}=7.0$ was kept constant throughout our calculations, which controls the size of the basis sets in calculations. The cutoff energy was chosen as - 6.0 Ry to separate valence and core states. The convergence criteria for charge and energy were set to be 1×10^{-4}eV and 1×10^{-4} Ry during self-consistency cycles, respectively.

3. Results and discussions

AFM topography images of samples treated by method Ⅰ and Ⅱ are presented in Figure 2(a)-(c) and (d)-(f), respectively. Smooth surfaces (RMS(sq)<0.5nm) are found on samples treated with 0.3% of method Ⅰ and 30% of method Ⅱ (Figure2(a) and (f)). Nanoscale corrugates with scale and density strongly dependent on the preparation method can be found on other samples (Figure 2(b)-(e)). In phase image shown Figure 2(g), with uncertainty of 5° to -5°, the corrugates show nearly same phase as the area nearby. Therefore, most of the observed corrugates in Figure 2(c) and (d) are assigned to the ripples of MoS_2, possibly induced by biaxial compressive strain inside the H_2O_2 adsorbed 1L-MoS_2(see Raman analysis in the following section). In Figure 2(c) and (d), we also observe some tall corrugates with much higher heights than the ripples nearby. Thus, these tall corrugates in Figure 2(c) and (d) may be the adsorbates from the ambient. Note that in Figure 2(b)-(e), most of scale of ripples and adsorbates are much smaller than the size of laser focus (~800nm). Thus in the following parts of this study, the PL and Raman spectra we obtain are an average signal of corrugates within the laser focus.

Raman spectra of samples prepared using method Ⅰ is shown in Figure 3(a). Two distinct Raman modes, i.e. A_{1g} at ~404 cm^{-1}(out of plane mode) and E_{2g}^{1}~385cm^{-1}(in plane mode) can be identified for all the three samples[18, 19]. The separation between two Raman peaks are calculated to be between 19-20cm^{-1}, which agrees with the distinct Raman feature of 1L-MoS_2[20]. In contrast to the Raman peaks of pristine 1L-MoS_2, blue shifts can be identified for both $A_{1g}$and E_{2g}^{1}peaks of the 1L-MoS_2 treated with method. As proposed by Rice et al[21], E_{2g}^{1} peak is much more sensitive than A_{1g} when strain is loaded on 1L-MoS_2. Blue (red) shift of E_{2g}^{1} mode indicates compressive(tensile) strain[21]. Moreover, according to the AFM topographic image in Figure 2, biaxial strain rather than uniaxial strain is expected in 1L-MoS_2. The blue shift of E_{2g}^{1} peak of 0.6, 1.0, 1.1cm^{-1} for samples treated with 0.3%, 3%, 30% using method Ⅰ indicates biaxial compressive strain with level of <0.2% in H_2O_2 treated 1L MoS_2[21-24]. According to the dependence of Raman A_{1g} shift on gate-voltage measured by Chakraboty[25], the blue (red) shift of A_{1g}indicates p(n)-type doping. Because the blue shift of A_{1g} caused by compressive strain is negligible[24] with the strain level of 0.2%, the blue shift of A_{1g} peak are all attributed to *p*-doping behavior of H_2O_2 molecules[25]. After compare the Raman shift to the dependence of A_{1g} shift vs gate voltage, the electron density in treated 1L-MoS_2 using method Ⅰ can be estimated to be 3-4$\times 10^{12}$ cm^{-2} using A_{1g} shift as 1.2-1.7cm^{-1} [25].

PL spectra of H_2O_2 treated 1L-MoS_2 using method Ⅰ are presented in Figure 3(b). Pronounced exciton bands are assigned to *B* exciton band (~ 2 eV), A^0 exciton

(neutral exciton, ~1.89 eV) and A^- exciton(trion, ~1.84 eV) [26]. It can be found that the PL intensity of 1L-MoS_2 is greatly enhanced by optimizing the amount of adsorbed H_2O_2. By using method Ⅰ with different concentrations of H_2O_2 (0.3%, 3%, 30%), the PL intensities of 1L-MoS_2 are enhanced by about 3.0, 4.69, 7.26 times, respectively. Prior to further analysis of enhancement mechanism, the influences of biaxial strain on the PL enhancement need to be discriminated as strain also affects the PL position and intensity[27-29]. Unlike biaxial tensile strain which enhances the PL of 1L-MoS_2[24], biaxial compressive strain is expected to reduce the PL intensity and induce blue shift of PL peak[27-29]. As indicated by Li et al, biaxial compressive strain with level of 0.2% only reduce the PL intensity by 10%[27, 29], which is much lower than the PL enhancement in our study. Therefore, the PL quenching induced by biaxial compressive strain is negligible.

The PL intensity of different excitons are also calculated and shown in Figure. 3(c). The intensity of neutral exciton is enhanced by up to 26.7 times for sample treated by 30% H_2O_2 (method Ⅰ) in contrast to that of pristine 1L-MoS_2. With the enhancement of neutral excitons, the PL intensities of trions are also enhanced by up to 3.6 times. This simultaneous enhancement of neutral exciton and trion had been observed and interpreted in our previous researches[30, 31] in which different p-type molecules are used to enhance the PL of 1L-MoS_2. In pristine 1L MoS_2, intrinsic defects such as sulphur vacancies are expected to generate mid-gap trapping states in the energy band, which further trap the carriers [32, 33] and induce a strong non-radiative recombination of the excitons. Like the passivation of surface defects in

quantum dots[34, 35], the intrinsic defects may be passivated with H_2O_2 molecules adsorbed on 1L-MoS_2[30]. The non-radiative recombination decay may be greatly suppressed and finally result in the enhanced radiative recombination rate of different excitons and their PL intensity[30]. Let k_{A^-} to be the decay rate of A^0 to A^-, and k_D to be the decay rate of A^0 and A^- to defect state(Figure 3(d)). The low PL quantum yield of pristine MoS_2 can be attributed to high k_{A^-} and k_D, both of which are ~0.5ps^{-1}[36]. However, for H_2O_2 passivated 1L-MoS_2, k_{A^-} may be reduced to 0.05 ps^{-1} - 0.1 ps^{-1} due to p-doping of H_2O_2 molecule. The adsorbtion of H_2O_2 molecules on 1L-MoS_2 attract electrons from MoS_2 and the non-radiative recombination via Auger process, $k_{i\_A^0}$, $k_{i\_A^-}$, are also diminished[13-15]. Due to the passivation effect, k_D may also be greatly reduced below 0.02 ps^{-1}, which finally results in the simultaneous PL enhancement of neutral exciton and trion.

Beside the PL enhancement, increasing blue shifts of B, A^0 and A^- excitons are also observed with the increasing doping concentration (Figure 3(e)). For 1L-MoS_2 sample treated by 30% solution(method Ⅰ) , maximum blue shifts for B, A^0 and A^- excitons are observed as 49, 8 and 14meV. Because the thickness of the adsorbed H_2O_2 on silicon is very thin, these blue shifts of excitons can be attributed to the modification of band structure (see the following calculation of band structure for details) rather than dielectric screening[37].

Raman and PL spectra of samples prepared using method Ⅱ are shown in Figure 3(f) and (g). For samples prepared by method Ⅱ, the decrease of E^1_{2g} shifts with different H_2O_2 concentration (Figure 3(f)) indicates compressive strain are

partially released. It's also worth to note that the PL intensity of samples prepared by method Ⅱ is much lower than method Ⅰ (shown in Figure 3(g)), which indicates PL quenching probably induced by over oxidation at high H_2O_2 concentration. Note that even for sample treated by 0.3% H_2O_2 using method Ⅱ, the dose of adsorbed H_2O_2 is expected to be higher than the samples prepared by method Ⅰ. Decreasing of PL intensity observed on samples treated with method Ⅱ (3% and 30%) can be attributed to extremely high concentration of H_2O_2, which may damage the lattice of 1-MoS_2 and finally quenches the PL intensity. Because of blue shift of A_{1g} peak is in contrary to that observed on suspended 1L MoS_2[38], the enhancement induced by suspending of 1L-MoS_2 is excluded. By comparing figure 3(b) to figure 3(f), we can conclude that method Ⅰ is desirable to prepare samples with strong enhancement.

In order to explain the blue shift of excitons, we calculate the electronic band structure of 1L-MoS_2 before and after adsorbtion of H_2O_2 molecule. A schematic of the H_2O_2 molecules on the 1L-MoS_2 is shown in Figure 4(a). It is found that the pristine 1L-MoS_2 shows a direct band gap of 1.93 eV at K point (Figure 4(b)), which is in good agreement with reported works[39, 40]. The structures for both valence band and conduction band of 1L-MoS_2 are not significantly altered by H_2O_2 (Figure 4(c)). Only a down shift of ~0.5eV of the whole band is observed. The band gap value is enlarged to be 1.97 eV with an increase by 40meV. This enlargement of band gap also induces blue shift of the energies of B exciton and A excitons , which agrees well with the blue shift of B excitons observed in Figure 3(e). Hence, the shift of excitons we observed in Figure 3(e) is attributed to the enlarged band structure. Two impurity

states emerge inside the band gap with the adsorbtion of H_2O_2, namely, one occupied state 490 meV above the top of valence band, one occupied state 27meV below the bottom of conduction band. Due to the instrumental restriction, the PL of excitons trapped into these two impurity states had not been observed in this study.

After understanding the role of H_2O_2 in the enhancement of 1L MoS_2, we further investigate the PL of 1L-MoS_2 treated by H_2O_2 and toluene, i.e. a sandwiched structure of H_2O_2/1L-MoS_2/toluene. As shown by AFM topographic image of H_2O_2/1L-MoS_2 treated by 10^{-6} mol/l toluene (Figure 5(a)), the surface of 1L-MoS_2 is fairly smooth, which agrees well with the high volatilization of toluene and also indicates low concentration of H_2O_2 molecules beneath 1L-MoS_2. Blue shift of Raman E^1_{2g} peak as 2.1 and 1.3 cm^{-1} with 10^{-6} and 10^{-9} mol/l of toluene (Figure 5(b)), respectively, indicates much stronger *p*-doping than the samples treated only by H_2O_2. With such strong p-doping, the PL intensity of 1L-MoS_2 is massively enhanced by up to 27.4 times in contrast to that of pristine MoS_2(Figure 5(c)). Because toluene and H_2O_2 molecules are adsorbed on separate sides of 1L-MoS_2, new p-type molecules containing –OH radicals are not likely to be formed, which excludes the PL enhancement from these new molecules. As aforementioned, H_2O_2 behaves as good molecule to passivate the defect on 1L-MoS_2. With the presence of toluene molecule and H_2O_2, the passivation effects may be enhanced to be even better than that obtained only with H_2O_2 molecules. From the quantum yield map (Figure 4(b)) of reference[30]), it can be estimated that k_A and k_D are reduced to <0.005 ps^{-1} , which results in strong PL with enhancement >25 times and quantum yield >12%. Detail

calculation of band structure of H_2O_2/1L-MoS_2/toluene is more complicated than H_2O_2/1L-MoS_2. The calculation and understanding of band perturbation is still ongoing and will be published in the future.

In summary, we show that the PL intensity of 1L-MoS_2 can be greatly enhanced up to 8 times by carefully selection the concentration and addition method of H_2O_2 molecules. The PL intensity of 1L-MoS_2 can be further enhanced by 27.4 times by using the sandwiched structure of H_2O_2/1L-MoS_2/toluene. The modification of 1L-MoS_2 with H_2O_2 molecular provides much wider control of light emission than conventional electric filed gating. Our study provides a simple and effective method, which benefits the potential application of 1L-MoS_2 in new optoelectronic devices.

Acknowledgements

The authors acknowledge the financial support from Natural Sciences Foundation of China (Grant No: 61306115 and 61178039) and China Postdoctoral Science Foundation (Granted No. 2013M541807). L. Y. acknowledges the support from Jiangsu Provincial Natural Science Foundation (Grant No. BK20140405) and XJTLU research development fund Grant No. PGRS-13-01-03.

References

1. R. S. Sundaram, M. Engel, A. Lombardo, R. Krupke, A. C. Ferrari, P. Avouris and M. Steiner, *Nano Letters*, 2013, **13**, 1416-1421.
2. O. Sanchez Lopez, E. A. Llado, V. Koman, A. F. Morral, A. Radenovic and K. Andras, *Acs Nano*, 2014, **8**, 3042-3047.
3. G.-H. Lee, Y.-J. Yu, X. Cui, N. Petrone, C.-H. Lee, M. S. Choi, D.-Y. Lee, C. Lee, W. J. Yoo, K. Watanabe, T. Taniguchi, C. Nuckolls, P. Kim and J. Hone, *Acs Nano*, 2013, **7**, 7931-7936.
4. B. Radisavljevic, A. Radenovic, J. Brivio, V. Giacometti and A. Kis, *Nature Nanotechnology*,

2011, **6**, 147-150.

5. Z. Yin, H. Li, H. Li, L. Jiang, Y. Shi, Y. Sun, G. Lu, Q. Zhang, X. Chen and H. Zhang, *Acs Nano*, 2012, **6**, 74-80.
6. M. Kin Fai, L. Changgu, J. Hone, S. Jie and T. F. Heinz, *Physical Review Letters*, 2010, **105**, 136805.
7. K. K. Kam and B. A. Parkinson, *Journal of Physical Chemistry*, 1982, **86**, 463-467.
8. A. Ramasubramaniam, *Physical Review B*, 2012, **86**, 115409.
9. A. Splendiani, L. Sun, Y. Zhang, T. Li, J. Kim, C.-Y. Chim, G. Galli and F. Wang, *Nano Letters*, 2010, **10**, 1271-1275.
10. D. Chen, Z. Wan, Y. Zhou, W. Xiang, J. Zhong, M. Ding, H. Yua and Z. Ji, *Journal of Materials Chemistry C*, 2015, **3**, 3141-3149.
11. R. Zhang, H. Lin, Y. Yu, D. Chen, J. Xu and Y. Wang, *Laser & Photonics Reviews*, 2014, **8**, 158-164.
12. A. Sobhani, A. Lauchner, S. Najmaei, C. Ayala-Orozco, F. Wen, J. Lou and N. J. Halas, *Applied Physics Letters*, 2014, **104**, 031112.
13. S. Mouri, Y. Miyauchi and K. Matsuda, *Nano Letters*, 2013, **13**, 5944-5948.
14. H. Nan, Z. Wang, W. Wang, Z. Liang, Y. Lu, Q. Chen, D. He, p. Tan, F. Miao, X. Wang, J. Wang and Z. Ni, *ACS Nano*, 2014, **8**, 5738-5745.
15. S. Tongay, J. Zhou, C. Ataca, J. Liu, J. S. Kang, T. S. Matthews, L. You, J. Li, J. C. Grossman and J. Wu, *Nano Letters*, 2013, **13**, 2831-2836.
16. J. Li, J. Wierzbowski, O. Ceylan, J. Klein, F. Nisic, A. Tuan Le, F. Meggendorfer, C.-A. Palma, C. Dragonetti, J. V. Barth, J. J. Finley and E. Margapoti, *Applied Physics Letters*, 2014, **105**, 241116.
17. P. Blaha, ed., *WIEN2k userguide, WIEN2k, An Augmented Plane Wave Plus Local Orbitals Program for Calculating Crystal Properties*, Vienna University of Technology, Austria, 2001.
18. C. Lee, H. Yan, L. E. Brus, T. F. Heinz, J. Hone and S. Ryu, *Acs Nano*, 2010, **4**, 2695-2700.
19. A. Molina-Sanchez and L. Wirtz, *Physical Review B*, 2011, **84**, 155413.
20. M. Buscema, A. G. Steele, S. J. v. d. H. Zant and A. Castellanos-Gomez, *Nano Research*, 2014, **7**, 561-571.
21. C. Rice, R. J. Young, R. Zan, U. Bangert, D. Wolverson, T. Georgiou, R. Jalil and K. S. Novoselov, *Physical Review B*, 2013, **87**, 081307.
22. H. J. Conley, B. Wang, J. I. Ziegler, R. F. Haglund, S. T. Pantelides and K. I. Bolotin, *Nano Letters*, 2013, **13**, 3626-3630.
23. E. Scalise, M. Houssa, G. Pourtois, V. V. Afanas′ ev and A. Stesmans, *Physica E: Low-dimensional Systems and Nanostructures*, 2014, **56**, 416-421.
24. H. Li, A. W. Contryman, X. Qian, S. M. Ardakani, Y. Gong, X. Wang, J. M. Weisse, C. H. Lee, J. Zhao, P. M. Ajayan, J. Li, H. C. Manoharan and X. Zheng, *Nature Communications*, 2015, **6**, 7381.
25. B. Chakraborty, A. Bera, D. V. S. Muthu, S. Bhowmick, U. V. Waghmare and A. K. Sood, *Physical Review B*, 2012, **85**, 161403.
26. K. F. Mak, K. He, C. Lee, G. H. Lee, J. Hone, T. F. Heinz and J. Shan, *Nature Materials*, 2013, **12**, 207-211.
27. F. Li, Y. Yan, B. Han, L. Li, X. Huang, M. Yao, Y. Gong, X. Jin, B. Liu, C. Zhu, Q. Zhou and T. Cui, *Nanoscale*, 2015, **7**, 9075-9082.

28. G. Plechinger, A. Castellanos-Gomez, M. Buscema, H. S. J. van der Zant, G. A. Steele, A. Kuc, T. Heine, C. Schueller and T. Korn, *2d Materials*, 2015, **2**,1
29. C. H. Li, local biaxial strain in MoS_2, http://l17.mit.edu/ ~sina/2D /LocalBiaxialStraininMoS2_Zheng.pdf).
30. W. Su, H. Dou, D. Huo, N. Dai and L. Yang, *Chemical Physics Letters*, 2015, **635**, 40-44.
31. W. Su, N. Kumar, N. Dai and D. Roy, *Nano Research*, 2015, **paper in publishing**.
32. H. Qiu, T. Xu, Z. Wang, W. Ren, H. Nan, Z. Ni, Q. Chen, S. Yuan, F. Miao, F. Song, G. Long, Y. Shi, L. Sun, J. Wang and X. Wang, *Nature Communications*, 2013, **4**, 2642.
33. W. Zhou, X. Zou, S. Najmaei, Z. Liu, Y. Shi, J. Kong, J. Lou, P. M. Ajayan, B. I. Yakobson and J.-C. Idrobo, *Nano Letters*, 2013, **13**, 2615-2622.
34. A. Puzder, A. J. Williamson, F. Gygi and G. Galli, *Physical Review Letters*, 2004, **92,**217401.
35. O. Voznyy, S. M. Thon, A. H. Ip and E. H. Sargent, *Journal of Physical Chemistry Letters*, 2013, **4**, 987-992.
36. H. Shi, R. Yan, S. Bertolazzi, J. Brivio, B. Gao, A. Kis, D. Jena, H. G. Xing and L. Huang, *Acs Nano*, 2013, **7**, 1072-1080.
37. Y. Lin, X. Ling, L. Yu, S. Huang, A. L. Hsu, Y.-H. Lee, J. Kong, M. S. Dresselhaus and T. Palacios, *Nano Letters*, 2014, **14**, 5569-5576.
38. N. Scheuschner, O. Ochedowski, A.-M. Kaulitz, R. Gillen, M. Schleberger and J. Maultzsch, *Physical Review B*, 2014, **89**, 125406.
39. K. Dolui, I. Rungger, C. Das Pemmaraju and S. Sanvito, *Physical Review B*, 2013, **88**, 075420.
40. Q. Yue, Z. Shao, S. Chang and J. Li, *Nanoscale Research Letters*, 2013, **8**, 425.

Captions of Figures

Figure 1 Schematic of H_2O_2 doping 1L-MoS_2 prepared by method Ⅰ (top panel) and method Ⅱ(bottom panel);

Figure 2 (a)-(c)typical AFM topographic images of sample prepared by method Ⅰ using H_2O_2 with concentration of 0.3%, 3%,30% , respectively; (d)-(f) typical AFM topographic images of sample prepared by method Ⅱ using H_2O_2 with concentration of 0.3%, 3%,30% , respectively; (g) Phase image obtained with topographic image of Figure 2(c), the inset shows the phase profile (most falls within $\pm 5^\circ$) along the dashed line, note the errors of the phase image is also $\pm 5^\circ$.

Figure 3 (a) Raman spectra of 1L-MoS_2 samples prepared by method Ⅰ; (b) Measured and deconvoluted PL spectra of 1L-MoS_2 prepared by method Ⅰ; (c) calculated intensity of neutral exciton and trion, and electron density of 1L-MoS_2 prepared by method Ⅰ; (d), exciton transition in 1L-MoS_2 with defect state(D, 1.8eV) involved. In this image Γ_{A^0} Γ_{A^-} and Γ_D are radiative decay rates of neutral exciton, trion and trapped excitons, respectively. k_{A^-} and $k_{D_{A^0}}$ are decay rates of A^0 to A^- and D, respectively. $k_{D_{A^-}}$ is decay rate from A^- to D. $k_{i\_A^0}$, $k_{i\_A^-}$ and k_{i_D} are non-radiative decay rates of A^0, A^- and trapped excitons related with carrier-phonon scattering & Auger process, respectively. (e), exciton energy of 1L-MoS_2 prepared by method Ⅰ; (f) PL and (g) Raman of 1L-MoS2 prepared by method Ⅱ.

Figure 4 (a) Side view (top panel) and top view(bottom panel) supercell of MoS_2 adsorbed with a H2O2 molecule; (b) band structure diagram of a pristine 1L MoS_2; (c) band structure diagram of 1L-MoS2 adsorbed with a H_2O_2 molecule;

Figure 5 (a) AFM topographic image of H_2O_2/1L-MoS_2/toluene with toluene of 10^{-6}mol/l; (b) Raman and (c) PL of H_2O_2/1L-MoS_2/toluene samples with different concentration of toluene.

Figures

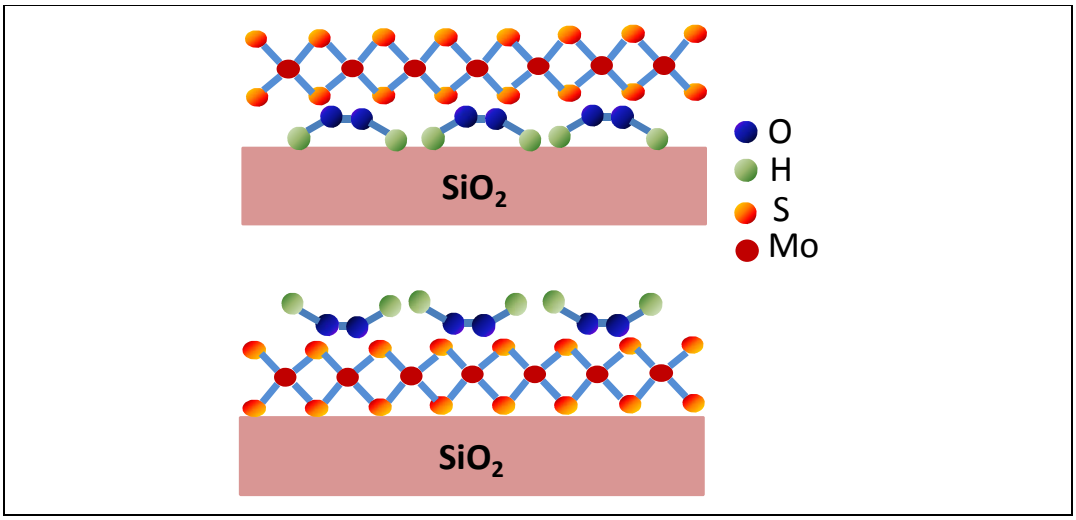

Figure 1 **Su et al**

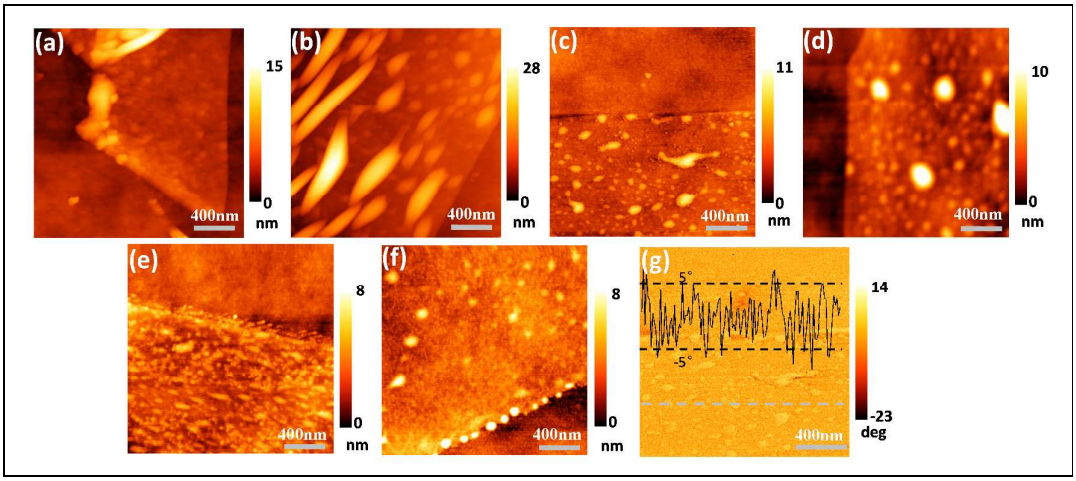

Figure 2 **Su et al**

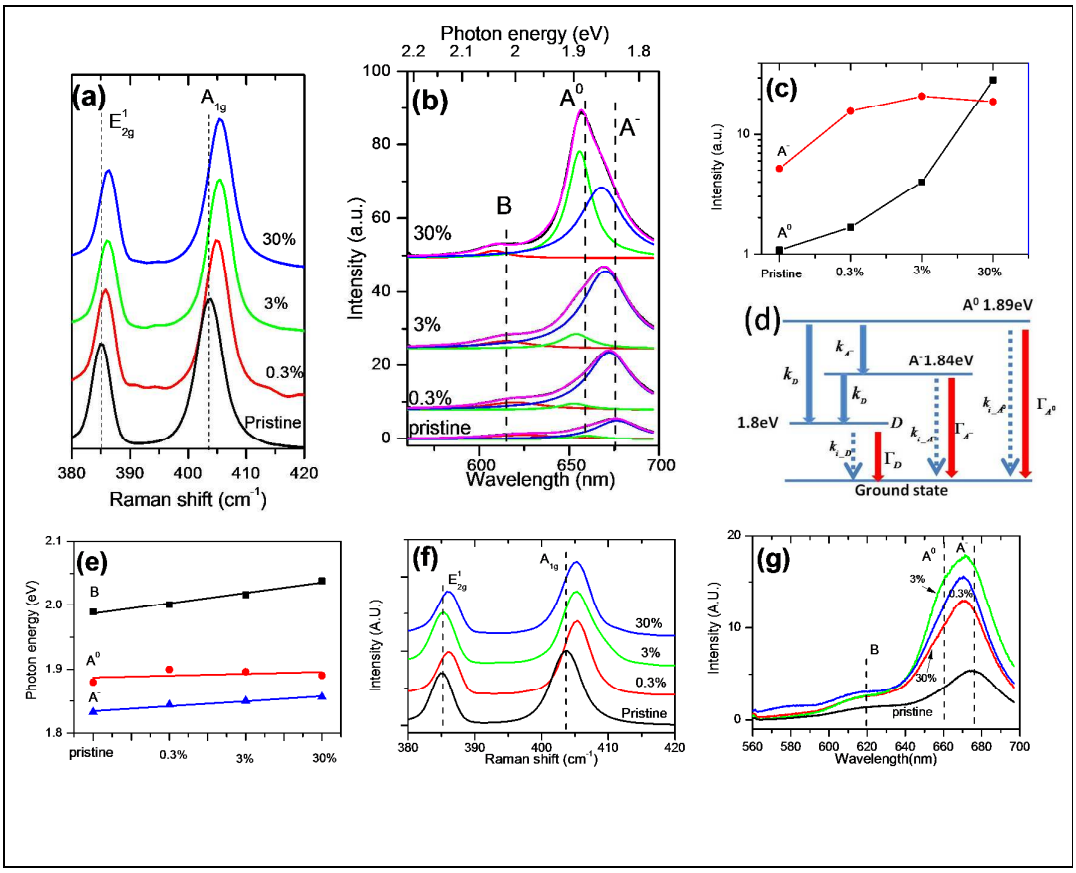

Figure 3 **Su et al**

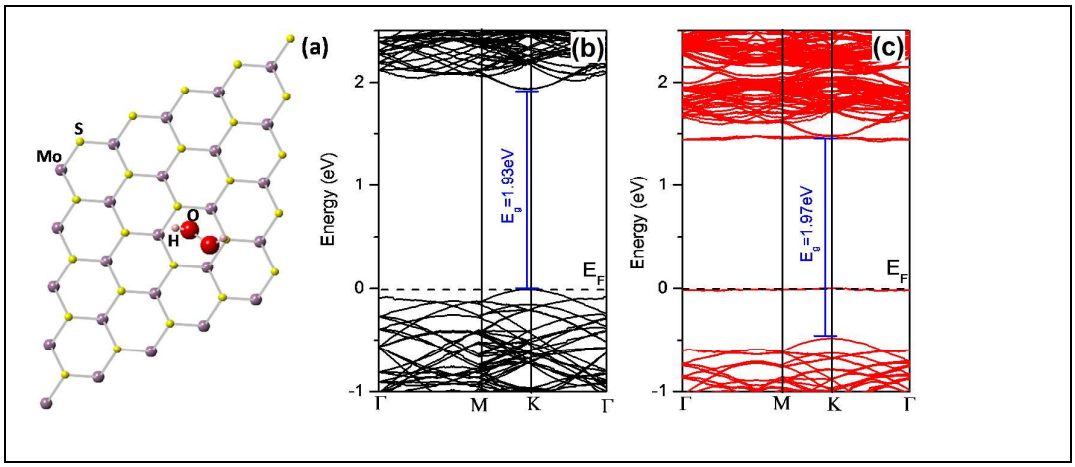

Figure 4 **Su et al**

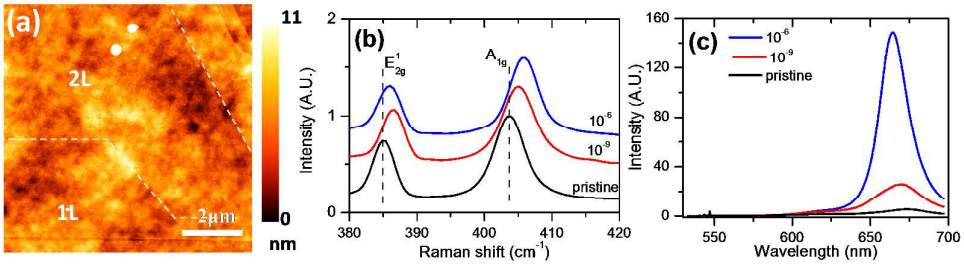

Figure 5 **Su et al**